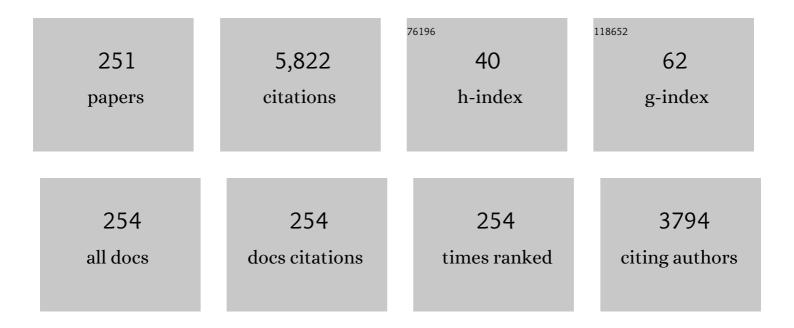
Satoshi Yamasaki

List of Publications by Year in descending order

Source: https://exaly.com/author-pdf/2523030/publications.pdf Version: 2024-02-01



#	Article	IF	CITATIONS
1	Optically detected magnetic resonance of nitrogen-vacancy centers in vertical diamond Schottky diodes. Japanese Journal of Applied Physics, 2022, 61, SC1061.	0.8	0
2	Selectively buried growth of heavily B doped diamond layers with step-free surfaces in N doped diamond (111) by homoepitaxial lateral growth. Applied Surface Science, 2022, , 153340.	3.1	1
3	Impact of nitrogen doping on homoepitaxial diamond (111) growth. Diamond and Related Materials, 2022, 125, 108997.	1.8	0
4	Study of ion-implanted nitrogen related defects in diamond Schottky barrier diode by transient photocapacitance and photoluminescence spectroscopy. Japanese Journal of Applied Physics, 2021, 60, SBBD07.	0.8	3
5	Carrier transport mechanism of diamond p ⁺ –n junction at low temperature using Schottky–pn junction structure. Japanese Journal of Applied Physics, 2021, 60, 030905.	0.8	5
6	Inversion channel MOSFET on heteroepitaxially grown free-standing diamond. Carbon, 2021, 175, 615-619.	5.4	9
7	Mechanical damage-free surface planarization of single-crystal diamond based on carbon solid solution into nickel. Diamond and Related Materials, 2021, 116, 108390.	1.8	1
8	Inversion-type p-channel diamond MOSFET issues. Journal of Materials Research, 2021, 36, 4688-4702.	1.2	13
9	Insight into temperature impact of Ta filaments on high-growth-rate diamond (100) films by hot-filament chemical vapor deposition. Diamond and Related Materials, 2021, 118, 108515.	1.8	8
10	Fabrication of inversion p-channel MOSFET with a nitrogen-doped diamond body. Applied Physics Letters, 2021, 119, .	1.5	11
11	Characterization of Schottky Barrier Diodes on Heteroepitaxial Diamond on 3C-SiC/Si Substrates. IEEE Transactions on Electron Devices, 2020, 67, 212-216.	1.6	11
12	Energy distribution of Al2O3/diamond interface states characterized by high temperature capacitance-voltage method. Carbon, 2020, 168, 659-664.	5.4	20
13	Vector Electrometry in a Wide-Gap-Semiconductor Device Using a Spin-Ensemble Quantum Sensor. Physical Review Applied, 2020, 14, .	1.5	17
14	Insight into Al2O3/B-doped diamond interface states with high-temperature conductance method. Applied Physics Letters, 2020, 117, .	1.5	11
15	Study of defects in diamond Schottky barrier diode by photocurrent spectroscopy. Japanese Journal of Applied Physics, 2020, 59, SGGK14.	0.8	2
16	Temperature dependence of diamond MOSFET transport properties. Japanese Journal of Applied Physics, 2020, 59, SGGD19.	0.8	4
17	Determination of Current Leakage Sites in Diamond p–n Junction. Physica Status Solidi (A) Applications and Materials Science, 2019, 216, 1900243.	0.8	1
18	Highâ€Rate Growth of Singleâ€Crystalline Diamond (100) Films by Hotâ€Filament Chemical Vapor Deposition with Tantalum Filaments at 3000 °C. Physica Status Solidi (A) Applications and Materials Science, 2019, 216, 1900244.	0.8	7

#	Article	IF	CITATIONS
19	Inversion channel mobility and interface state density of diamond MOSFET using N-type body with various phosphorus concentrations. Applied Physics Letters, 2019, 114, .	1.5	19
20	Conductive-probe atomic force microscopy and Kelvin-probe force microscopy characterization of OH-terminated diamond (111) surfaces with step-terrace structures. Japanese Journal of Applied Physics, 2019, 58, SIIB08.	0.8	5
21	Highâ€Rate Growth of Singleâ€Crystalline Diamond (100) Films by Hotâ€Filament Chemical Vapor Deposition with Tantalum Filaments at 3000 °C. Physica Status Solidi (A) Applications and Materials Science, 2019, 216, 1970071.	0.8	1
22	Charge-state control of ensemble of nitrogen vacancy centers by n–i–n diamond junctions. Applied Physics Express, 2018, 11, 033004.	1.1	10
23	Single crystal diamond membranes for nanoelectronics. Nanoscale, 2018, 10, 4028-4035.	2.8	27
24	Anisotropic diamond etching through thermochemical reaction between Ni and diamond in high-temperature water vapour. Scientific Reports, 2018, 8, 6687.	1.6	41
25	Direct observation of inversion capacitance in p-type diamond MOS capacitors with an electron injection layer. Japanese Journal of Applied Physics, 2018, 57, 04FR01.	0.8	14
26	Temperature dependence of electrical characteristics for diamond Schottky-pn diode in forward bias. Diamond and Related Materials, 2018, 85, 49-52.	1.8	11
27	Formation of atomically flat hydroxyl-terminated diamond (1 1 1) surfaces via water vapor annealing. Applied Surface Science, 2018, 458, 222-225.	3.1	23
28	Reverseâ€recovery of diamond pâ€iâ€n diodes. IET Power Electronics, 2018, 11, 695-699.	1.5	4
29	Direct Nanoscale Sensing of the Internal Electric Field in Operating Semiconductor Devices Using Single Electron Spins. ACS Nano, 2017, 11, 1238-1245.	7.3	82
30	Fabrication of graphene on atomically flat diamond (111) surfaces using nickel as a catalyst. Diamond and Related Materials, 2017, 75, 105-109.	1.8	22
31	Mechanism of anisotropic etching on diamond (111) surfaces by a hydrogen plasma treatment. Applied Surface Science, 2017, 422, 452-455.	3.1	22
32	Dynamic properties of diamond high voltage p–i–n diodes. Japanese Journal of Applied Physics, 2017, 56, 04CR14.	0.8	10
33	Diamond Schottky-pn diode using lightly nitrogen-doped layer. Diamond and Related Materials, 2017, 75, 152-154.	1.8	37
34	Estimation of Inductively Coupled Plasma Etching Damage of Boronâ€Doped Diamond Using Xâ€Ray Photoelectron Spectroscopy. Physica Status Solidi (A) Applications and Materials Science, 2017, 214, 1700233.	0.8	11
35	Observation of Interface Defects in Diamond Lateral p-n-Junction Diodes and Their Effect on Reverse Leakage Current. IEEE Transactions on Electron Devices, 2017, 64, 3298-3302.	1.6	6
36	High-Temperature Bipolar-Mode Operation of Normally-Off Diamond JFET. IEEE Journal of the Electron Devices Society, 2017, 5, 95-99.	1.2	27

#	Article	IF	CITATIONS
37	Influence of substrate misorientation on the surface morphology of homoepitaxial diamond (111) films. Physica Status Solidi (A) Applications and Materials Science, 2016, 213, 2051-2055.	0.8	10
38	N-type control of single-crystal diamond films by ultra-lightly phosphorus doping. Applied Physics Letters, 2016, 109, .	1.5	49
39	Magnetic Resonance Imaging Bone Edema at Enrollment Predicts Rapid Radiographic Progression in Patients with Early RA: Results from the Nagasaki University Early Arthritis Cohort. Journal of Rheumatology, 2016, 43, 1278-1284.	1.0	14
40	Pure negatively charged state of the NV center in <mml:math xmlns:mml="http://www.w3.org/1998/Math/MathML"><mml:mi>n</mml:mi>-type diamond. Physical Review B, 2016, 93, .</mml:math 	1.1	77
41	Inversion channel diamond metal-oxide-semiconductor field-effect transistor with normally off characteristics. Scientific Reports, 2016, 6, 31585.	1.6	150
42	Diamond electronics. , 2016, , .		2
43	Normally-Off Diamond Junction Field-Effect Transistors With Submicrometer Channel. IEEE Electron Device Letters, 2016, 37, 209-211.	2.2	36
44	Desorption time of phosphorus during MPCVD growth of n-type (001) diamond. Diamond and Related Materials, 2016, 64, 208-212.	1.8	11
45	Heavily phosphorus-doped nano-crystalline diamond electrode for thermionic emission application. Diamond and Related Materials, 2016, 63, 165-168.	1.8	23
46	Defect luminescence in Diamond and GaN: towards single photon emitting devices. , 2016, , .		0
47	Potential profile evaluation of a diamond lateral p–n junction diode using Kelvin probe force microscopy. Physica Status Solidi (A) Applications and Materials Science, 2015, 212, 2589-2594.	0.8	1
48	Fabrication of diamond lateral p–n junction diodes on (111) substrates. Physica Status Solidi (A) Applications and Materials Science, 2015, 212, 2548-2552.	0.8	7
49	Electronic properties of diamond Schottky barrier diodes fabricated on silicon-based heteroepitaxially grown diamond substrates. Applied Physics Express, 2015, 8, 104103.	1.1	30
50	Upregulation of Thrombospondin 1 Expression in Synovial Tissues and Plasma of Rheumatoid Arthritis: Role of Transforming Growth Factor-1²1 toward Fibroblast-like Synovial Cells. Journal of Rheumatology, 2015, 42, 943-947.	1.0	21
51	Electrical excitation of silicon-vacancy centers in single crystal diamond. Applied Physics Letters, 2015, 106, .	1.5	33
52	Germanium-Vacancy Single Color Centers in Diamond. Scientific Reports, 2015, 5, 12882.	1.6	251
53	Realization of Atomically Controlled Diamond Surfaces. Journal of the Japan Society for Precision Engineering, 2014, 80, 433-438.	0.0	0
54	Large improvement of phosphorus incorporation efficiency in n-type chemical vapor deposition of diamond. Applied Physics Letters, 2014, 105, .	1.5	23

#	Article	IF	CITATIONS
55	Atomistic mechanism of perfect alignment of nitrogen-vacancy centers in diamond. Applied Physics Letters, 2014, 105, .	1.5	39
56	Carrier transport in homoepitaxial diamond films with heavy phosphorus doping. Japanese Journal of Applied Physics, 2014, 53, 05FP05.	0.8	19
57	Observation of negative electron affinity in low-voltage discharging boron-doped polycrystalline diamond. Japanese Journal of Applied Physics, 2014, 53, 05FP09.	0.8	4
58	Generation and transportation mechanisms for two-dimensional hole gases in GaN/AlGaN/GaN double heterostructures. Journal of Applied Physics, 2014, 115, .	1.1	42
59	Direct first-principles simulation of a high-performance electron emitter: Lithium-oxide-coated diamond surface. Journal of Applied Physics, 2014, 116, .	1.1	6
60	Electron emission from nitrogen-containing diamond with narrow-gap coplanar electrodes. Japanese Journal of Applied Physics, 2014, 53, 05FP08.	0.8	0
61	Diamond electronic devices fabricated using heavily doped hopping p ⁺ and n ⁺ layers. Japanese Journal of Applied Physics, 2014, 53, 05FA12.	0.8	29
62	Investigation of electron emission site of p–i–n diode-type emitters with negative electron affinity. Japanese Journal of Applied Physics, 2014, 53, 05FP07.	0.8	0
63	Analysis of selective growth of n-type diamond in lateral p–n junction diodes by cross-sectional transmission electron microscopy. Japanese Journal of Applied Physics, 2014, 53, 05FP01.	0.8	10
64	Polarizationâ€controlled dressedâ€photon–phonon etching of patterned diamond structures. Physica Status Solidi (A) Applications and Materials Science, 2014, 211, 2339-2342.	0.8	7
65	Doping and interface of homoepitaxial diamond for electronic applications. MRS Bulletin, 2014, 39, 499-503.	1.7	49
66	Unique temperature dependence of deep ultraviolet emission intensity for diamond light emitting diodes. Japanese Journal of Applied Physics, 2014, 53, 05FP02.	0.8	4
67	600 V Diamond Junction Field-Effect Transistors Operated at 200\$^{circ}{m C}\$. IEEE Electron Device Letters, 2014, 35, 241-243.	2.2	74
68	Perfect selective alignment of nitrogen-vacancy centers in diamond. Applied Physics Express, 2014, 7, 055201.	1.1	84
69	Reduction of nâ€ŧype diamond contact resistance by graphite electrode. Physica Status Solidi - Rapid Research Letters, 2014, 8, 137-140.	1.2	16
70	Energy-loss mechanism of single-crystal silicon microcantilever due to surface defects generated during plasma processing. Journal of Micromechanics and Microengineering, 2013, 23, 065020.	1.5	9
71	Electrical characterization of diamond Pi <scp>N</scp> diodes for high voltage applications. Physica Status Solidi (A) Applications and Materials Science, 2013, 210, 2035-2039.	0.8	52
72	Light penetration depth dependence of photocarrier life time and the Hall effect in phosphorous-doped and boron-doped homoepitaxial CVD diamond films. Diamond and Related Materials, 2013, 33, 49-53.	1.8	0

#	Article	IF	CITATIONS
73	Fabrication of bipolar junction transistor on (001)-oriented diamond by utilizing phosphorus-doped n-type diamond base. Diamond and Related Materials, 2013, 34, 41-44.	1.8	38
74	Single photon, spin, and charge in diamond semiconductor at room temperature. , 2013, , .		0
75	Early diagnosis and treatment for remission of clinically amyopathic dermatomyositis complicated by rapid progress interstitial lung disease: a report of two cases. Modern Rheumatology, 2013, 23, 190-194.	0.9	21
76	Diamond foam electrodes for electrochemical applications. Electrochemistry Communications, 2013, 33, 88-91.	2.3	57
77	Tunable light emission from nitrogen-vacancy centers in single crystal diamond PIN diodes. Applied Physics Letters, 2013, 102, .	1.5	62
78	<i>Ab initio</i> dynamics of field emission from diamond surfaces. Applied Physics Letters, 2013, 103, .	1.5	8
79	High-Temperature Operation of Diamond Junction Field-Effect Transistors With Lateral p-n Junctions. IEEE Electron Device Letters, 2013, 34, 1175-1177.	2.2	51
80	Takayasu arteritis developing during treatment of ulcerative colitis with infliximab. Modern Rheumatology, 2013, 23, 572-576.	0.9	6
81	An elderly patient with chronic active Epstein–Barr virus infection with mixed cryoglobulinemia and review of the literature. Modern Rheumatology, 2013, 23, 1022-1028.	0.9	4
82	High-Voltage Vacuum Switch with a Diamond p–i–n Diode Using Negative Electron Affinity. Japanese Journal of Applied Physics, 2012, 51, 090113.	0.8	17
83	High serum matrix metalloproteinase 3 is characteristic of patients with paraneoplastic remitting seronegative symmetrical synovitis with pitting edema syndrome. Modern Rheumatology, 2012, 22, 584-588.	0.9	35
84	Unique Properties of Diamond and Its Device Applications. Hyomen Kagaku, 2012, 33, 634-638.	0.0	0
85	lsotope Effect of Deuterium Microwave Plasmas on the Formation of Atomically Flat (111) Diamond Surfaces. Japanese Journal of Applied Physics, 2012, 51, 090106.	0.8	4
86	Formation of Step-Free Surfaces on Diamond (111) Mesas by Homoepitaxial Lateral Growth. Japanese Journal of Applied Physics, 2012, 51, 090107.	0.8	19
87	Diamond bipolar junction transistor device with phosphorus-doped diamond base layer. Diamond and Related Materials, 2012, 27-28, 19-22.	1.8	51
88	Device Design of Diamond Schottky-pn Diode for Low-Loss Power Electronics. Japanese Journal of Applied Physics, 2012, 51, 090116.	0.8	6
89	Nonlinear behavior of currentâ€dependent emission for diamond lightâ€emitting diodes. Physica Status Solidi (A) Applications and Materials Science, 2012, 209, 1754-1760.	0.8	13
90	Diamond Junction Field-Effect Transistors with Selectively Grown n\$^{+}\$-Side Gates. Applied Physics Express, 2012, 5, 091301.	1.1	61

#	Article	IF	CITATIONS
91	Maskless Selective Growth Method for p–n Junction Applications on (001)-Oriented Diamond. Japanese Journal of Applied Physics, 2012, 51, 090118.	0.8	6
92	Electrical properties of lateral p–n junction diodes fabricated by selective growth of n ⁺ diamond. Physica Status Solidi (A) Applications and Materials Science, 2012, 209, 1761-1764.	0.8	32
93	Isotope Effect of Deuterium Microwave Plasmas on the Formation of Atomically Flat (111) Diamond Surfaces. Japanese Journal of Applied Physics, 2012, 51, 090106.	0.8	2
94	Formation of Step-Free Surfaces on Diamond (111) Mesas by Homoepitaxial Lateral Growth. Japanese Journal of Applied Physics, 2012, 51, 090107.	0.8	19
95	High-Voltage Vacuum Switch with a Diamond p–i–n Diode Using Negative Electron Affinity. Japanese Journal of Applied Physics, 2012, 51, 090113.	0.8	22
96	Device Design of Diamond Schottky-pn Diode for Low-Loss Power Electronics. Japanese Journal of Applied Physics, 2012, 51, 090116.	0.8	5
97	Maskless Selective Growth Method for p–n Junction Applications on (001)-Oriented Diamond. Japanese Journal of Applied Physics, 2012, 51, 090118.	0.8	5
98	Disease activity score 28 may overestimate the remission induction of rheumatoid arthritis patients treated with tocilizumab: comparison with the remission by the clinical disease activity index. Modern Rheumatology, 2011, 21, 365-369.	0.9	27
99	Reduction in serum levels of substance P in patients with rheumatoid arthritis by etanercept, a tumor necrosis factor inhibitor. Modern Rheumatology, 2011, 21, 244-250.	0.9	17
100	Energy level of compensator states in (001) phosphorus-doped diamond. Diamond and Related Materials, 2011, 20, 1016-1019.	1.8	20
101	Multiple phosphorus chemical sites in heavily phosphorus-doped diamond. Applied Physics Letters, 2011, 98, .	1.5	16
102	Cageâ€5haped Borate Esters with Tris(2â€oxyphenyl)methane or â€silane System Frameworks Bearing Multiple Tuning Factors: Geometric and Substituent Effects on Their Lewis Acid Properties. Chemistry - A European Journal, 2011, 17, 3856-3867.	1.7	26
103	Effects of the anti-interleukin-6 receptor antibody, tocilizumab, on serum lipid levels in patients with rheumatoid arthritis. Rheumatology International, 2011, 31, 451-456.	1.5	100
104	Carrier transport of diamond p ⁺ â€iâ€n ⁺ junction diode fabricated using lowâ€resistance hopping p ⁺ and n ⁺ layers. Physica Status Solidi (A) Applications and Materials Science, 2011, 208, 937-942.	0.8	5
105	Misorientation-angle dependence of boron incorporation into (001)-oriented chemical-vapor-deposited (CVD) diamond. Journal of Crystal Growth, 2011, 317, 60-63.	0.7	90
106	CD4+CD25 ^{high} CD127 ^{low/-} Treg Cell Frequency from Peripheral Blood Correlates with Disease Activity in Patients with Rheumatoid Arthritis. Journal of Rheumatology, 2011, 38, 2517-2521.	1.0	74
107	Enhancement in emission efficiency of diamond deep-ultraviolet light emitting diode. Applied Physics Letters, 2011, 99, .	1.5	73
108	A case of Sjögren syndrome with pulmonary amyloidosis complicating microscopic polyangiitis. Modern Rheumatology, 2011, 21, 646-650.	0.9	3

#	Article	IF	CITATIONS
109	In rheumatoid arthritis patients treated with tocilizumab, the rate of clinical disease activity index (CDAI) remission at 24 weeks is superior in those with higher titers of IgM-rheumatoid factor at baseline. Modern Rheumatology, 2011, 21, 370-374.	0.9	16
110	Contribution of an adenine to guanine single nucleotide polymorphism of the matrix metalloproteinase-13 (MMP-13) â''77 promoter region to the production of anticyclic citrullinated peptide antibodies in patients with HLA-DRB1*shared epitope-negative rheumatoid arthritis. Modern Rheumatology, 2011, 21, 240-243.	0.9	1
111	Disease activity score 28 may overestimate the remission induction of rheumatoid arthritis patients treated with tocilizumab: comparison with the remission by the clinical disease activity index. Modern Rheumatology, 2011, 21, 365-369.	0.9	14
112	Cutaneous vasculitis induced by TNF inhibitors: a report of three cases. Modern Rheumatology, 2010, 20, 86-89.	0.9	37
113	Switching to the anti-interleukin-6 receptor antibody tocilizumab in rheumatoid arthritis patients refractory to antitumor necrosis factor biologics. Modern Rheumatology, 2010, 20, 40-45.	0.9	11
114	Improvement of (001)-oriented diamond p-i-n diode by use of selective grown n+ layer. Physica Status Solidi (A) Applications and Materials Science, 2010, 207, 2099-2104.	0.8	12
115	Diamond Schottkyâ€pn diode without tradeâ€off relationship between onâ€resistance and blocking voltage. Physica Status Solidi (A) Applications and Materials Science, 2010, 207, 2105-2109.	0.8	34
116	Electron Emission from a Diamond (111) p–i–n+Junction Diode with Negative Electron Affinity during Room Temperature Operation. Applied Physics Express, 2010, 3, 041301.	1.1	24
117	Plasma-Induced Deterioration of Mechanical Characteristics of Microcantilever. Japanese Journal of Applied Physics, 2010, 49, 04DL20.	0.8	16
118	High-Performance Three-Terminal Fin Field-Effect Transistors Fabricated by a Combination of Damage-Free Neutral-Beam Etching and Neutral-Beam Oxidation. Japanese Journal of Applied Physics, 2010, 49, 04DC17.	0.8	11
119	Growth of atomically step-free surface on diamond {111} mesas. Diamond and Related Materials, 2010, 19, 288-290.	1.8	33
120	Mechanism of mechanical deterioration in silicon microcantilever induced by plasma process. , 2010, , .		0
121	Switching to the anti-interleukin-6 receptor antibody tocilizumab in rheumatoid arthritis patients refractory to antitumor necrosis factor biologics. Modern Rheumatology, 2010, 20, 40-45.	0.9	13
122	Electron Emission from Diamond (111) p+-i-n+ Junction Diode. Materials Research Society Symposia Proceedings, 2009, 1203, 1.	0.1	0
123	Prediction of DAS28-CRP remission in patients with rheumatoid arthritis treated with tacrolimus at 6 months by baseline variables. Modern Rheumatology, 2009, 19, 652-656.	0.9	6
124	Prediction of DAS28-ESR remission at 6 months by baseline variables in patients with rheumatoid arthritis treated with etanercept in Japanese population. Modern Rheumatology, 2009, 19, 488-492.	0.9	20
125	Diamond Schottky p–n diode with high forward current density. Physica Status Solidi (A) Applications and Materials Science, 2009, 206, 2086-2090.	0.8	20
126	Diamond Schottky-pn diode with high forward current density and fast switching operation. Applied Physics Letters, 2009, 94, .	1.5	77

Satoshi Yamasaki

#	Article	IF	CITATIONS
127	Flattening of oxidized diamond (111) surfaces with H2SO4/H2O2 solutions. Diamond and Related Materials, 2009, 18, 213-215.	1.8	12
128	Selective Growth of Buried n+Diamond on (001) Phosphorus-Doped n-Type Diamond Film. Applied Physics Express, 2009, 2, 055502.	1.1	55
129	Development of Low-AC-Loss Bi-2223 Superconducting Multifilamentary Wires. IEEE Transactions on Applied Superconductivity, 2009, 19, 3053-3056.	1.1	11
130	Electrical and light-emitting properties from (111)-oriented homoepitaxial diamond p–i–n junctions. Diamond and Related Materials, 2009, 18, 764-767.	1.8	18
131	Characterization of specific contact resistance on heavily phosphorus-doped diamond films. Diamond and Related Materials, 2009, 18, 782-785.	1.8	35
132	Hall effect of photocurrent in CVD diamond film. Diamond and Related Materials, 2009, 18, 779-781.	1.8	2
133	High performance of diamond p+-i-n+ junction diode fabricated using heavily doped p+ and n+ layers. Applied Physics Letters, 2009, 94, .	1.5	73
134	Prediction of DAS28-ESR remission at 6Âmonths by baseline variables in patients with rheumatoid arthritis treated with etanercept in Japanese population. Modern Rheumatology, 2009, 19, 488-492.	0.9	19
135	Electrical and lightâ€emitting properties of homoepitaxial diamond p–i–n junction. Physica Status Solidi (A) Applications and Materials Science, 2008, 205, 2200-2206.	0.8	29
136	Electrical activity of doped phosphorus atoms in (001) nâ€ŧype diamond. Physica Status Solidi (A) Applications and Materials Science, 2008, 205, 2195-2199.	0.8	29
137	Fermi level pinning-free interface at metals/homoepitaxial diamond (111) films after oxidation treatments. Applied Physics Letters, 2008, 92, 112112.	1.5	14
138	Homoepitaxial diamond p–n+ junction with low specific on-resistance and ideal built-in potential. Diamond and Related Materials, 2008, 17, 782-785.	1.8	23
139	Low specific contact resistance of heavily phosphorus-doped diamond film. Applied Physics Letters, 2008, 93, .	1.5	68
140	Atomically flat diamond (111) surface formation by homoepitaxial lateral growth. Diamond and Related Materials, 2008, 17, 1051-1054.	1.8	43
141	Roughening of atomically flat diamond (111) surfaces by a hot HNO3/H2SO4 solution. Diamond and Related Materials, 2008, 17, 486-488.	1.8	14
142	Mapping of extended defects in B-doped (001) homoepitaxial diamond films by electron-beam-induced current (EBIC) and cathodoluminescence (CL) combination technique. Diamond and Related Materials, 2008, 17, 489-493.	1.8	5
143	Generation and reduction in SiO2/Si interface state density during plasma etching processes. Journal of Applied Physics, 2008, 104, 063308.	1.1	14
144	Exciton-derived Electron Emission from (001) Diamond <i>p</i> – <i>n</i> Junction Diodes with Negative Electron Affinity. Applied Physics Express, 2008, 1, 015004.	1.1	8

#	Article	IF	CITATIONS
145	Total Photoelectron Emission Yield Spectroscopy on Diamond Surfaces. Hyomen Kagaku, 2008, 29, 151-158.	0.0	Ο
146	n-Type Diamond Growth by Phosphorus Doping. Materials Research Society Symposia Proceedings, 2007, 1039, 1.	0.1	2
147	Low-damage fabrication of high aspect nanocolumns by using neutral beams and ferritin-iron-core mask. Journal of Vacuum Science & Technology B, 2007, 25, 760.	1.3	11
148	Hillock-Free Heavily Boron-Doped Homoepitaxial Diamond Films on Misoriented (001) Substrates. Japanese Journal of Applied Physics, 2007, 46, 1469-1470.	0.8	28
149	Etching Damage in Diamond Studied Using an Energy-Controlled Oxygen Ion Beam. Japanese Journal of Applied Physics, 2007, 46, 60-64.	0.8	9
150	Surface roughening of diamond (001) films during homoepitaxial growth in heavy boron doping. Diamond and Related Materials, 2007, 16, 767-770.	1.8	37
151	Electrical and light-emitting properties of (001)-oriented homoepitaxial diamond p–i–n junction. Diamond and Related Materials, 2007, 16, 1025-1028.	1.8	18
152	Surface electronic properties on boron doped (111) CVD homoepitaxial diamond films after oxidation treatments. Diamond and Related Materials, 2007, 16, 831-835.	1.8	6
153	The role of boron atoms in heavily boron-doped semiconducting homoepitaxial diamond growth — Study of surface morphology. Diamond and Related Materials, 2007, 16, 409-411.	1.8	11
154	Carrier compensation in (001) n-type diamond by phosphorus doping. Diamond and Related Materials, 2007, 16, 796-799.	1.8	40
155	n-type diamond growth by phosphorus doping on (0 0 1)-oriented surface. Journal Physics D: Applied Physics, 2007, 40, 6189-6200.	1.3	90
156	Growth and characterization of boron-doped CVD homoepitaxial diamond films. Journal of Crystal Growth, 2007, 299, 235-242.	0.7	4
157	Electrical and optical characterizations of (001)-oriented homoepitaxial diamond p–n junction. Diamond and Related Materials, 2006, 15, 513-516.	1.8	15
158	N-type doping on (001)-oriented diamond. Diamond and Related Materials, 2006, 15, 548-553.	1.8	20
159	Surface conductive layers on (111) diamonds after oxygen treatments. Diamond and Related Materials, 2006, 15, 692-697.	1.8	20
160	Cage-Shaped Borate Esters with Enhanced Lewis Acidity and Catalytic Activity. Organic Letters, 2006, 8, 761-764.	2.4	40
161	Ab initio energetics of phosphorus impurity in subsurface regions of hydrogenated diamond surfaces. E-Journal of Surface Science and Nanotechnology, 2006, 4, 124-128.	0.1	5
162	Emission properties from dense exciton gases in diamond. Physica Status Solidi (A) Applications and Materials Science, 2006, 203, 3226-3244.	0.8	21

#	Article	IF	CITATIONS
163	Ab initio energetics of phosphorus related complex defects in synthetic diamond. Physica B: Condensed Matter, 2006, 376-377, 304-306.	1.3	16
164	Hydrogen plasma etching mechanism on (001) diamond. Journal of Crystal Growth, 2006, 293, 311-317.	0.7	24
165	Energetics of dopant atoms in subsurface positions of diamond semiconductor. Superlattices and Microstructures, 2006, 40, 574-579.	1.4	4
166	High-Efficiency Excitonic Emission with Deep-Ultraviolet Light from (001)-Oriented Diamondp-i-nJunction. Japanese Journal of Applied Physics, 2006, 45, L1042-L1044.	0.8	52
167	Photoelectron Emission Mechanism From Hydrogen Terminated Nano-Crystalline Diamond. Materials Research Society Symposia Proceedings, 2006, 956, 1.	0.1	3
168	Surface reactions during etching of organic low-k films by plasmas of N2 and H2. Journal of Applied Physics, 2006, 99, 083305.	1.1	40
169	Thermodynamic theory for efficiency of multiple impurity-atom doping in diamond. Physica Status Solidi A, 2005, 202, 2134-2140.	1.7	4
170	Growth and characterization of phosphorus-doped diamond using organophosphorus gases. Physica Status Solidi A, 2005, 202, 2122-2128.	1.7	22
171	Diamond Schottky barrier diodes with low specific on-resistance. Semiconductor Science and Technology, 2005, 20, 1203-1206.	1.0	5
172	Reduction of plasma-induced damage in SiO[sub 2] films during pulse-time-modulated plasma irradiation. Journal of Vacuum Science & Technology an Official Journal of the American Vacuum Society B, Microelectronics Processing and Phenomena, 2005, 23, 389.	1.6	27
173	In vacuo measurements of dangling bonds created during Ar-diluted fluorocarbon plasma etching of silicon dioxide films. Applied Physics Letters, 2005, 86, 264104.	1.5	20
174	Surface conductive layers on oxidized (111) diamonds. Applied Physics Letters, 2005, 87, 262107.	1.5	19
175	Efficiency of multiple atom doping in wide band gap semiconductors. Applied Physics Letters, 2005, 86, 261910.	1.5	9
176	Ohmic contacts on p-type homoepitaxial diamond and their thermal stability. Semiconductor Science and Technology, 2005, 20, 860-863.	1.0	44
177	Growth of phosphorus-doped diamond using tertiarybutylphosphine and trimethylphosphine as dopant gases. Diamond and Related Materials, 2005, 14, 340-343.	1.8	20
178	Passivation effects of deuterium exposure on boron-doped CVD homoepitaxial diamond. Diamond and Related Materials, 2005, 14, 2023-2026.	1.8	9
179	n-type conductivity of phosphorus-doped homoepitaxial single crystal diamond on (001) substrate. Diamond and Related Materials, 2005, 14, 2007-2010.	1.8	18
180	Effect of rapid sample cooling on efficiency of multiple impurity-atom doping. Diamond and Related Materials, 2005, 14, 2039-2042.	1.8	1

#	Article	IF	CITATIONS
181	Strong Excitonic Emission from (001)-Oriented DiamondP-NJunction. Japanese Journal of Applied Physics, 2005, 44, L1190-L1192.	0.8	22
182	Electrical and optical characterization of boron-doped (111) homoepitaxial diamond films. Diamond and Related Materials, 2005, 14, 1964-1968.	1.8	21
183	n-type doping of (001)-oriented single-crystalline diamond by phosphorus. Applied Physics Letters, 2005, 86, 222111.	1.5	172
184	Hyperfine Interaction of Nitrogen Donor in 4H-SiC Studied by Pulsed-ENDOR. Materials Science Forum, 2005, 483-485, 351-354.	0.3	2
185	Local Dielectric Degradation of Cu-Contaminated SiO ₂ Thin Films. Solid State Phenomena, 2004, 95-96, 641-646.	0.3	1
186	Leakage Current Distribution and Dielectric Breakdown of Cu-Contaminated Thin SiO[sub 2]. Journal of the Electrochemical Society, 2004, 151, F81.	1.3	4
187	Atomic-layer resolved monitoring of thermal oxidation of Si(001) by reflectance difference oscillation technique. Thin Solid Films, 2004, 455-456, 759-763.	0.8	12
188	Position-Specified Formation of Epitaxial Si Grains on Thermally Oxidized Si(001) Surfaces via Isolated Nanodots. Chemistry of Materials, 2004, 16, 3518-3523.	3.2	3
189	Indium-Catalyzed Direct Chlorination of Alcohols Using Chlorodimethylsilaneâ^'Benzil as a Selective and Mild System. Journal of the American Chemical Society, 2004, 126, 7186-7187.	6.6	92
190	Electron-spin phase relaxation of phosphorus donors in nuclear-spin-enriched silicon. Physical Review B, 2004, 70, .	1.1	89
191	Local Electrical Properties of Non-Doped Polycrystalline Silicon Thin-Films Evaluated Using Conductive Atomic Force Microscopy. Solid State Phenomena, 2003, 93, 339-344.	0.3	2
192	Conductive-Mode Atomic Force Microscopy Study of Amorphous Silicon Nitride Thin Films. Japanese Journal of Applied Physics, 2003, 42, L1321-L1323.	0.8	3
193	Topography and Local Electrical Properties of Nondoped Polycrystalline Silicon Thin Films Evaluated Using Conductive-Mode Atomic Force Microscopy. Japanese Journal of Applied Physics, 2003, 42, L1302-L1304.	0.8	1
194	Leakage Current Distribution of Cu-Contaminated Thin SiO2. Japanese Journal of Applied Physics, 2003, 42, L160-L162.	0.8	11
195	In-situ Electron-spin-resonance Observation of Creation and Annihilation of Surface Dangling Bonds. Hyomen Kagaku, 2003, 24, 648-655.	0.0	0
196	Origin of type-Cdefects on theSi(100)â^'(2×1)surface. Physical Review B, 2002, 65, .	1.1	38
197	In vacuo electron-spin-resonance study on amorphous fluorinated carbon films for understanding of surface chemical reactions in plasma etching. Applied Physics Letters, 2002, 81, 1773-1775.	1.5	9
198	EPR Study of Single Silicon Vacancy-Related Defects in 4H- and 6H-SiC. Materials Science Forum, 2002, 389-393, 497-500.	0.3	3

12

#	Article	IF	CITATIONS
199	ESR Characterization of SiC Bulk Crystals and SiO ₂ /SiC Interface. Materials Science Forum, 2002, 389-393, 1025-1028.	0.3	13
200	Observation of oscillating behavior in the reflectance difference spectra of oxidized Si(001) surfaces. Journal of Applied Physics, 2002, 91, 3637-3643.	1.1	19
201	Direct observation of surface dangling bonds during plasma process: chemical reactions during H2 and Ar plasma treatments. Thin Solid Films, 2002, 407, 139-143.	0.8	6
202	Electron Spin Resonance Observation of the Si(111)-(7×7)Surface and Its Oxidation Process. Physical Review Letters, 2001, 86, 1054-1057.	2.9	22
203	Scanning Probe Microscopy and Lithography of Ultrathin Si3N4Films Grown on Si(111) and Si(001). Japanese Journal of Applied Physics, 2001, 40, 4368-4372.	0.8	5
204	In situ electron spin resonance observation of Si(111) 7×7 surface during hydrogenation process. Journal of Vacuum Science & Technology an Official Journal of the American Vacuum Society B, Microelectronics Processing and Phenomena, 2001, 19, 1898.	1.6	4
205	Local structure of Ge nanoislands on Si(111) surfaces with a SiO2 coverage. Applied Physics Letters, 2001, 78, 2563-2565.	1.5	47
206	Chlorosilane adsorption on clean Si surfaces: Scanning tunneling microscopy and Fourier-transform infrared absorption spectroscopy studies. Journal of Vacuum Science and Technology A: Vacuum, Surfaces and Films, 2001, 19, 2001-2006.	0.9	10
207	Surface Microchemical Reactions during Hydrogenated Silicon Growth Studied by In-situ ESR Technique. Materials Research Society Symposia Proceedings, 2000, 609, 111.	0.1	5
208	Fast In-diffusion of Hydrogen at the Initial Stage of Hydrogen Plasma Treatment on a-Si:H Films Observed by In-situ ESR Measurements. Materials Research Society Symposia Proceedings, 2000, 609, 2651.	0.1	0
209	In situ electron spin resonance of initial oxidation processes of Si surfaces. Applied Surface Science, 2000, 162-163, 299-303.	3.1	7
210	Effects of Chemical Composition and Morphology of Substrate Surfaces on Crystallinity of Ultrathin Hydrogenated Microcrystalline Silicon Films. Japanese Journal of Applied Physics, 2000, 39, 6647-6651.	0.8	8
211	Microscopic origin of light-induced ESR centers in undoped hydrogenated amorphous silicon. Physical Review B, 2000, 62, 15702-15710.	1.1	13
212	Creation and annihilation mechanism of dangling bonds within the a-Si:H growth surface studied by in situ ESR technique. Journal of Non-Crystalline Solids, 2000, 266-269, 529-533.	1.5	19
213	Control of crystallinity of microcrystalline silicon film grown on insulating glass substrates. Journal of Non-Crystalline Solids, 1998, 227-230, 857-860.	1.5	32
214	Comparative Evaluation of Ultrathin Mask Layers of SiO2, SiOxNyand SiNxfor Selective Area Growth of Si. Japanese Journal of Applied Physics, 1998, 37, 4204-4208.	0.8	11
215	Selective Area Growth of Si on Thin Insulating Layers for Nanostructure Fabrication. Japanese Journal of Applied Physics, 1998, 37, L1087-L1089.	0.8	8
216	Probing the Elementary Surface Reactions of Hydrogenated Silicon PECVD by In-situ ESR. Materials Research Society Symposia Proceedings, 1998, 536, 463.	0.1	3

#	Article	IF	CITATIONS
217	Growth of amorphous-layer-free microcrystalline silicon on insulating glass substrates by plasma-enhanced chemical vapor deposition. Applied Physics Letters, 1997, 71, 1534-1536.	1.5	46
218	In situelectron-spin-resonance measurements of film growth of hydrogenated amorphous silicon. Applied Physics Letters, 1997, 70, 1137-1139.	1.5	32
219	Spatial distribution of phosphorus atoms surrounding spin centers of P-doped hydrogenated amorphous silicon elucidated by pulsed ESR. Journal of Non-Crystalline Solids, 1996, 198-200, 330-333.	1.5	0
220	STM and Raman study of the evolution of the surface morphology in μc-Si:H. Journal of Non-Crystalline Solids, 1996, 198-200, 863-866.	1.5	9
221	Hydrogen-Initiated Nucleation and Growth of Hydrogenated Amorphous Silicon on Graphite. Japanese Journal of Applied Physics, 1995, 34, L379-L381.	0.8	2
222	Substrate Temperature Dependence of Deuteron Bonding States in Deuterated Amorphous Silicon Studied by2HNuclear Magnetic Resonance. Japanese Journal of Applied Physics, 1994, 33, 5668-5670.	0.8	3
223	Nucleation and coalescence in hydrogenated amorphous silicon studied by scanning tunneling microscopy. Applied Physics Letters, 1994, 65, 1760-1762.	1.5	24
224	Pulsed-ESR study of light-induced metastable defect in a-Si:H. Journal of Non-Crystalline Solids, 1993, 164-166, 169-174.	1.5	69
225	1H Nuclear Magnetic Resonance Study of Hydrogenated Amorphous Silicon Deposited from a Xe-diluted Silane Plasma. Japanese Journal of Applied Physics, 1992, 31, 989-994.	0.8	1
226	Light-induced defects in phosphorus-doped hydrogenated amorphous silicon. Journal of Non-Crystalline Solids, 1992, 141, 176-187.	1.5	4
227	Control of photodegradation in amorphous silicon: The effect of deuterium. The Philosophical Magazine: Physics of Condensed Matter B, Statistical Mechanics, Electronic, Optical and Magnetic Properties, 1991, 63, 281-292.	0.6	18
228	2D and1H Nuclear Magnetic Resonance Study of Deuterated Amorphous Silicon and Partially Deuterated Hydrogenated Amorphous Silicon. Japanese Journal of Applied Physics, 1991, 30, 1909-1914.	0.8	6
229	Structural Differences between Hydrogenated and Deuterated Amorphous Silicon Films Prepared by Plasma-Enhanced Chemical Vapor Deposition. Japanese Journal of Applied Physics, 1991, 30, L142-L144.	0.8	7
230	1H Nuclear Magnetic Resonance Study of Hydrogen Distribution in Partially Deuterated Hydrogenated Amorphous Silicon. Japanese Journal of Applied Physics, 1991, 30, L541-L543.	0.8	4
231	The Staebler-Wronski Effect on Defect Luminescence in Hydrogenated Amorphous Silicon. Japanese Journal of Applied Physics, 1989, 28, L1086-L1088.	0.8	2
232	Nuclear-magnetic-resonance study of amorphous silicon-hydrogen-phosphorus alloys. Physical Review B, 1988, 38, 31-38.	1.1	9
233	Optical absorption edge of hydrogenated amorphous silicon studied by photoacoustic spectroscopy. The Philosophical Magazine: Physics of Condensed Matter B, Statistical Mechanics, Electronic, Optical and Magnetic Properties, 1987, 56, 79-97.	0.6	90
234	31P Nuclear Magnetic Resonance Study of Local Bonding Configuration of Phosphorus in Amorphous Silicon-Hydrogen-Phosphorus Alloys. Japanese Journal of Applied Physics, 1987, 26, L2041-L2043.	0.8	5

#	Article	IF	CITATIONS
235	Si29nuclear magnetic resonance of amorphous hydrogenated silicon and amorphous microcrystalline mixed-phase hydrogenated silicon. Physical Review B, 1987, 35, 4581-4590.	1.1	13
236	Silicon-29 Nuclear Magnetic Resonance Study of Amorphous-Microcrystalline Mixed-Phase Hydrogenated Silicon. Japanese Journal of Applied Physics, 1986, 25, L313-L315.	0.8	4
237	Interpretation of29Si nuclear magnetic resonance spectra of amorphous hydrogenated silicon. Journal of Applied Physics, 1986, 60, 1839-1841.	1.1	19
238	Proton nuclear magnetic resonance study on hydrogen incorporation in amorphousâ€microcrystalline mixedâ€phase hydrogenated silicon. Journal of Applied Physics, 1984, 56, 2658-2663.	1.1	18
239	NMR study of μc-Si:H. Journal of Non-Crystalline Solids, 1983, 59-60, 779-782.	1.5	13
240	Endor study of a-Si:H. Journal of Non-Crystalline Solids, 1983, 59-60, 141-144.	1.5	3
241	Gap-State Profiles of a-Si: H Deduced from Below-Gap Optical Absorption. Japanese Journal of Applied Physics, 1982, 21, L539-L541.	0.8	34
242	(Invited) Optical, Electrical and Structural Properties of Plasma-Deposited Amorphous Silicon. Japanese Journal of Applied Physics, 1981, 20, 267.	0.8	27
243	A Photoluminescence Study of Amorphous-Microcrystalline Mixed-Phase Si:H Films. Japanese Journal of Applied Physics, 1981, 20, L793-L796.	0.8	15
244	Structural Study on Amorphous-Microcrystalline Mixed-Phase Si:H Films. Japanese Journal of Applied Physics, 1981, 20, L439-L442.	0.8	45
245	Boron Doping of Hydrogenated Silicon Thin Films. Japanese Journal of Applied Physics, 1981, 20, L183-L186.	0.8	80
246	Determination of the Optical Constants of Thin Films Using Photoacoustic Spectroscopy. Japanese Journal of Applied Physics, 1981, 20, L665-L668.	0.8	40
247	A New Model for the Carrier Transport in Amorphous Si: H Schottky Barrier Diodes. Japanese Journal of Applied Physics, 1980, 19, 131.	0.8	8
248	Electrical and Structural Properties of Phosphorous-Doped Glow-Discharge Si:F:H and Si:H Films. Japanese Journal of Applied Physics, 1980, 19, L305-L308.	0.8	189
249	Self-Heating Effects in Long Superconducting Thin Films over a Wide Temperature Range. Japanese Journal of Applied Physics, 1979, 18, 667-670.	0.8	16
250	Nanometer Scale Height Standard Using Atomically Controlled Diamond Surface. Applied Physics Express, 0, 2, 055001.	1.1	20
251	Calculation of Lattice Constant of 4H-SiC as a Function of Impurity Concentration. Materials Science Forum, 0, 645-648, 247-250.	0.3	25